

A new discrete-time Robust Adaptive Predictive Control-based RMRAC applied to grid connected converters with LCL Filter

Um novo controlador preditivo robusto adaptativo baseado em RMRAC em tempo discreto aplicado a conversores conectados à rede com filtro LCL

DOI:10.34117/bjdv7n3-053

Recebimento dos originais: 08/02/2021
Aceitação para publicação: 01/03/2021

Wagner Barreto da Silveira

Master Degree Student on Electrical Engineering
Federal University of Santa Maria, Santa Maria, Brazil
Endereço: Av. Roraima nº 1000 Cidade Universitária Bairro - Camobi, Santa Maria -
RS, 97105-900
E-mail: wasilveira91@hotmail.com

Deise Maria Cirolini Milbradt

Doctor Degree Candidate on Electrical Engineering
Federal University of Santa Maria, Santa Maria, Brazil
Endereço: Av. Roraima nº 1000 Cidade Universitária Bairro - Camobi, Santa Maria -
RS, 97105-900
E-mail: deise.milbradt@ufsm.br

Guilherme Vieira Hollweg

Doctor Degree Candidate on Electrical Engineering
Federal University of Santa Maria, Santa Maria, Brazil
Endereço: Av. Roraima nº 1000 Cidade Universitária Bairro - Camobi, Santa Maria -
RS, 97105-900
E-mail: guilhermehollweg@gmail.com

Paulo Jefferson Dias de Oliveira Evald

Doctor on Electrical Engineering
Franciscan University
Endereço: R. Silva Jardim, 1323 - Nossa Sra. do Rosario, Santa Maria - RS, 97010-492
E-mail: paulo.evald@gmail.com

Rodrigo Varella Tambara

Doctor on Electrical Engineering
Federal University of Santa Maria, Santa Maria, Brazil
Endereço: Av. Roraima nº 1000 Cidade Universitária Bairro - Camobi, Santa Maria
- RS, 97105-900
E-mail: rodvarella10@gmail.com

Hilton Abílio Gründling

Doctor on Electronic and Computer Engineering
Federal University of Santa Maria, Santa Maria, Brazil

Endereço: Av. Roraima nº 1000 Cidade Universitária Bairro - Camobi, Santa Maria
- RS, 97105-900
E-mail: ghilton03@gmail.com

ABSTRACT

In this work, is developed a new discrete-time robust adaptive predictive control based on combining the adaptive structure of a Model Reference Adaptive Controller (MRAC), to adjust gains online, with the control law One Sample Ahead Preview (OSAP), a particular case of deadbeat controller, for the current loop of a grid-connected voltage-source converter, also, this control not need resonant controllers to reject exogenous disturbances. A case application is presented, the grid-side currents control of a three-phase full-bridge static converter connected to the electrical grid by LCL filter. Simulation results are presented to show the performance of the proposed controller in a grid connected system.

Keywords: Adaptive Control, Robust Control, Model Predictive Control, OSAP Control, Grid-Connected Converters, LCL Filter.

RESUMO

Neste trabalho, um novo controle preditivo robusto adaptativo em tempo discreto é desenvolvido, combinando a estrutura adaptativa do Model Reference Adaptive Control (MRAC), para ajustar os ganhos online, com a lei de controle One Sample Ahead Preview (OSAP), um caso particular do controlador Deadbeat, para a malha de controle da corrente de um conversor alimentado a tensão conectado à rede, cujo controlador resultante não requer controladores ressonantes para rejeitar distúrbios exógenos. Uma aplicação de caso é apresentada, o controle de correntes do lado da rede de um conversor estático trifásico em ponte completa conectado à rede elétrica por um filtro LCL. Os resultados da simulação são apresentados para mostrar o desempenho do controlador proposto em um sistema conectado à rede.

Palavras-chave: Controle Adaptativo, Controle Robusto, Controle por Modelo Preditivo, Controle OSAP, Conversores Conectados à Rede, Filtro LCL.

1 INTRODUCTION

The fast development of the human society and the industrial production implies on intense demand for energy and fast fossil fuels depletion Chen et al. (2019); Fang et al. (2019). Furthermore, concerns about well-being of the environment and global warming have attracted interest in deployments of renewable energy sources Malinowski et al. (2015); Jha (2016); Chowdhury (2016); Costa et al. (2020). Thus, since last decade, renewable energy sector has been turning more and more relevant Kuznietsov et al. (2019).

Grid-connected power generation systems based on photovoltaic panels, wind turbines, fuel cells, among others, have used static converters with LCL filters to attenuate high harmonic frequencies Dannehl et al. (2007). For high power converters, larger than

1MW, LCL filters are commonly employed due to their high attenuation of current harmonics, inherent to converter's switching frequency. In addition, without significantly increasing the reactive power consumed at the grid frequency compared to an L filter. Furthermore, the grid impedance causes uncertainties on LCL's resonance frequency. It is a relevant dynamic that have to be considered on controller design to ensure stability and performance of the grid-connected converter Liserre et al. (2006).

As for LCL resonance damping, there are two main solutions presented on literature, to suppress it. They are: (I) the use of passive damping to attenuate the resonance peak, which is undesirable at high power systems, due to energy cost and power losses caused by insertion of passive elements on the filter. Moreover, these methods depend on the PCC (Point of Common Coupling) characteristics; (II) the use of active damping, which can be achieved through different control strategies, such as optimal controller Mariethoz et al. (2008), PI controller Lindgren and Svensson (1998) and Ponnaluri and Serpa (2008), the PI controller with resonant Liserre et al. (2006), robust control Gabe et al. (2009) and Maccari (2014) and adaptive control Massing et al. (2012); Tambara et al. (2013).

Regardless of the approach used or the control technique, it's desirable the control algorithm has the following property: capable to keep system stability and good performance even in the presence of structured and unstructured uncertainties, as well as disturbances, since the performance and stability of the closed loop system is substantially dependent on the grid parameters and the dynamics of the converter output filter.

Ioannou and Tsakalis (1986a) shows a few strategies of RMRAC controller which has been used for a lot of papers along the years to solve similar problems of grid connected converters with LCL-filter. In Tambara (2014) proposed a RMRAC discrete-time feedback state and input-output approach controller based on a modified RLS (Recursive Least Square) adaptation algorithm, to damping of the resonant peak of the LCL filter. In addition, Evald et. al (2021) and Hollweg et al. (2020) presented a robust adaptive PI controller and a RMRAC and adaptive Super Twisting control method for grid-connected converters with LCL filter in a weak grid scenario.

Recently, among these new control schemes, predictive control such as model predictive control (MPC) Exposto et al. (2015) appears to be a very interesting alternative to obtain high performance for grid-connected inverter application. In Mohamed and El-Saadany (2007), an improved deadbeat current control scheme with a novel adaptive self-tuning load model for a three-phase pulse width- modulated (PWM) voltage-source

inverter is proposed. Baek et al. (2015); Shi et al. (2019) present a predictive current control method and its application to a voltage source inverter. In fact, these algorithms show good results if the system is well known. By the way, if the system presents structured and unstructured uncertainties (such as unmodeled dynamics) modifications must be included in these control schemes.

In order to meet the control requirements of the high- power static converter with LCL filter, this paper proposes a discrete time controller based on combining the adaptive structure of an RMRAC with the One Sample Ahead Preview (OSAP) control law, a particular case of a one step forward MPC controller, for the current loop of a voltage source converter connected to the grid.

2 GRID-CONNECTED CONVERTER WITH LCL

Conversion and electrical energy control by using power converters are important topics of research today. This is due the fact of the increasing energy demands and new requirements in terms of power quality and efficiency.

The renewable energy system is described by the natural source of power, converter, AC filter and capacitor bank. In Fig. 1, the complete system is presented. Here, it's represented renewable energy power system as a continuous- voltage source. Furthermore, it's approximated the grid to a sinusoidal source v_d in series with an inductance L_{g2} and parasitic resistance R_{g2} , assuming that it is predominantly inductive. In addition, LCL filter is represented by the Thevenin equivalent in relation to the PCC (Point of Common Coupling) Tambara et al. (2017). Their parameters, shown on Fig. 1, are i_c , v_c and i_g are converter- side currents, capacitor voltage and grid-side currents, respectively. In addition, C , L_g and R_g are the capacitance of the LCL filter and total grid-side inductance and total grid resistance, respectively.

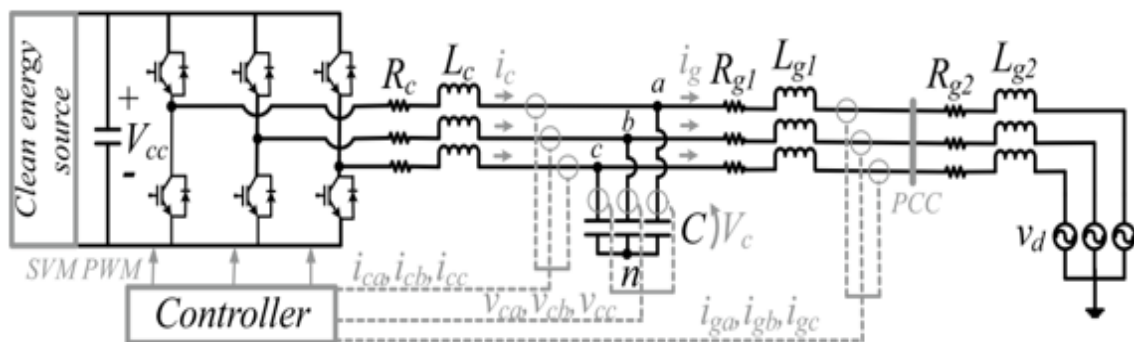


Fig. 1: Grid-tied converter with LCL filter
Source: Authors

The grid-connected converter by LCL filter model is highly coupled if it's considered a representation in abc coordinates Ewald, Tambara and Gründling (2020). Design a control method for coupled systems is a complex task. Moreover, if the plant has uncertainties and is subjected to parametric variations, it turns harder the control design. Then, here, the Clarke Transform Duesterhoeft et al. (1951) was applied on abc coordinates three-phase coupled model, obtaining two identical decoupled single-phase models in $\alpha\beta 0$ coordinates, Tambara et al. (2017). The equivalent circuits of single-phase models are shown on Fig. 2. These models are linear time-invariant (LIT) and assuming that grid phases are balanced, then the 0 axis can be disregarded, once there will be no path for current flow.

$$T_{\alpha\beta} = \begin{bmatrix} 1 & -1/2 & -1/2 \\ 0 & \sqrt{3}/2 & -\sqrt{3}/2 \\ 1/2 & 1/2 & 1/2 \end{bmatrix} \quad (1)$$

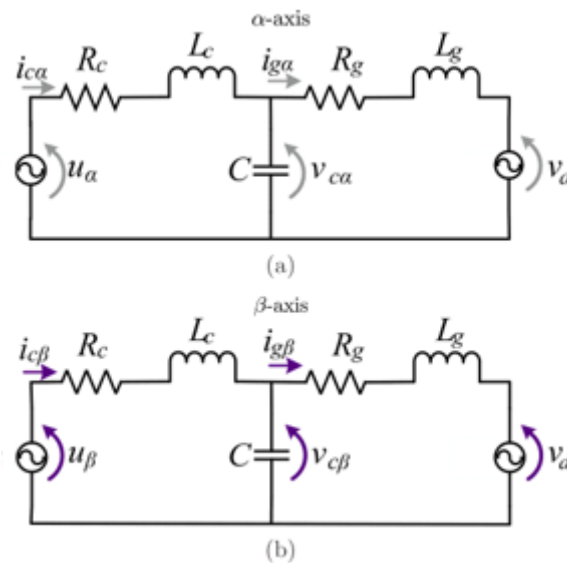


Fig. 2: Equivalent circuit of grid-connected voltage-fed three-phase converter with LCL filter: (a) α axis, (b) β axis filter
Source: Authors

The identical decoupled single-phase models, $G(s)$, considering $V_d = 0$,

$$G(s) = \frac{i_g(s)}{u(s)} = \frac{1}{L_g L_c C} \frac{1}{s^2 + \frac{R_g L_c + R_c L_g}{L_g L_c} s + \frac{(L_c + L_g + R_c R_g C)}{L_g L_c C} s + \frac{R_g + R_c}{L_g L_c C}} \quad (2)$$

where $u(s)$ is the voltage synthesized by converter. To do it, a Space Vector Modulation (SVM) was implemented. Moreover, digital implementation delay was considered in the simulation and modelled as a 1 step time delay on control action.

3 CONTROL STRUCTURE AND ADAPTATION ALGORITHM

Considering a linear, time-invariant SISO plant:

$$G(z) = G_c(z)[1 + \mu\Delta_m(z)] + \mu\Delta_a(z) \quad (3)$$

and $G_0(z)$ as

$$G_0(z) = k_p \frac{z_0}{R_0} \quad (4)$$

and a model reference in the form

$$W_m(z) = \frac{b_m}{z - a_m} = \frac{y_m(z)}{r(z)} \quad (5)$$

from (1), it's defines a reduced model of the LCL Filter as

$$G_0(z) = \frac{b}{z - a} = \frac{y(z)}{u(z)} \quad (6)$$

whose values of a and b describe the dynamic of plant's real pole.

Rewriting (6) being

$$zy(z) - ay(z) = bu(z) \quad (7)$$

which implementable form results in

$$y(k + 1) = ay(k) + bu(k) \quad (8)$$

or

$$y(k) = ay(k - 1) + bu(k - 1) \quad (9)$$

From (8), it's desired to obtain a relation whose control law is able to match the plant output with the reference model output: $y(k + 1) = y_m(k + 1)$, so

$$u(k) = \frac{y(k+1) - ay(k)}{b} \quad (10)$$

Introducing (9) in (11), and replacing $y(k + 1)$ by $y_m(k + 1)$

$$u(k) = \frac{y_m(k+1) - a(ay(k-1) + bu(k-1))}{b} \quad (11)$$

As shown in (7), rewrites (5) as being:

$$y_m(k + 1) = a_m y_m(k) + b_m r(k) \quad (12)$$

Rewriting (12) in (11) and organizing the terms, it obtains,

$$\frac{b}{b_m} u(k) - \frac{ab}{b_m} u(k - 1) - \frac{a^2}{b_m} y(k - 1) + \frac{a_m}{b_m} y(k - 1) + \frac{a_m}{b_m} y_m(k) y_m(k) + r(k) = 0 \quad (13)$$

No loss of generality, consider $b_m = 1$ and replacing the coefficients that multiply the internal signals of the system by adaptive gains θ , it achieves the following control law:

$$\theta_1 u(k) + \theta_2 u(k - 1) + \theta_3 y(k - 1) + \theta_4 y_m(k) + r(k) = 0 \quad (14)$$

thence,

$$\theta^T(k) \omega(k) + r(k) = 0 \quad (15)$$

For rejection of exogenous disturbance, it is necessary to include in the control law, phase voltage signals $V_s(k)$ and quadrature $V_c(k)$, these components are described by

$$V_s(k) = A_s \sin(\omega_{ds} k T_s + f_s) \quad (16)$$

and

$$V_c(k) = A_c \sin(\omega_{dc} k T_s + f_c) \quad (17)$$

where A , ω_d and f are amplitude, frequency and phase of $V_s(k)$ and $V_c(k)$ components, respectively. Therefore, the equation (14), turns

$$\theta_1 u(k) + \theta_2 u(k - 1) + \theta_3 y(k - 1) + \theta_4 y_m(k) + \theta_5 V_s(k) + \theta_6 V_c(k) + r(k) = 0 \quad (18)$$

Then, for (15), it is update to

$$\omega(k) = [u(k) \ u(k - 1) \ y(k - 1) \ y_m(k) \ V_s(k) \ V_c(k)]$$

and

$$\theta^T(k) = [\theta_1(k) \ \theta_2(k) \ \theta_3(k) \ \theta_4(k) \ \theta_5(k) \ \theta_6(k)]$$

The parametric adaptation law used to tune online the gains of this proposed controller is the Gradient algorithm, similar to Ioannou and Tsakalis (1986b)

$$\theta(k+1) = (I - s\Gamma T_s)\theta(k) - T_s \kappa \frac{\Gamma \zeta(k) \epsilon_1(k)}{m^{-2}(k)} \quad (19)$$

where Γ is a positive symmetric matrix gain given as γI , κ is a positive scalar gain, the tracking error $e_1 = y - y_m$, augmented error $\epsilon_1 = e_1 + \theta^T \zeta - W_m(\theta^T \omega)$, $\zeta = W_m l \omega$ is a regression vector whose signals of vector $\omega(k)$ is filtered by reference model and

$$m^{-2}(k) = m^2(k) + \zeta^T(k) \Gamma \zeta(k) \quad (20)$$

where the majorant signal $m(k)$ it's calculated as

$$m(k+1) = (1 - T_s \delta_0) m(k) + T_s \delta_1 (|u(k)| + |y(k)|) \quad (21)$$

where $m(0) \geq \delta_1 / (1 - \delta_0)$. Moreover, the σ -modification, Ioannou and Tsakalis (1986a) is also used in the adaptation law, is given as follows,

$$\sigma(k) = \begin{cases} 0 & \text{if } \|\theta(k)\| < M_0 \\ \sigma_0 \left(\frac{\|\theta(k)\|}{M_0} - 1 \right) & \text{if } M_0 \leq \|\theta(k)\| \leq 2M_0 \\ \sigma_0 & \text{if } \|\theta(k)\| > 2M_0 \end{cases} \quad (22)$$

where σ_0 is the maximum value of $\sigma(k)$, M_0 is an upper bound of $\|\theta^*\|$ and $M_0 > 2\|\theta^*\|$. As usual, the value of $\|\theta(k)\|$ is unknown, M_0 is chosen large enough.

The control and adaptive structure block diagram proposed is shown on Fig. 3.

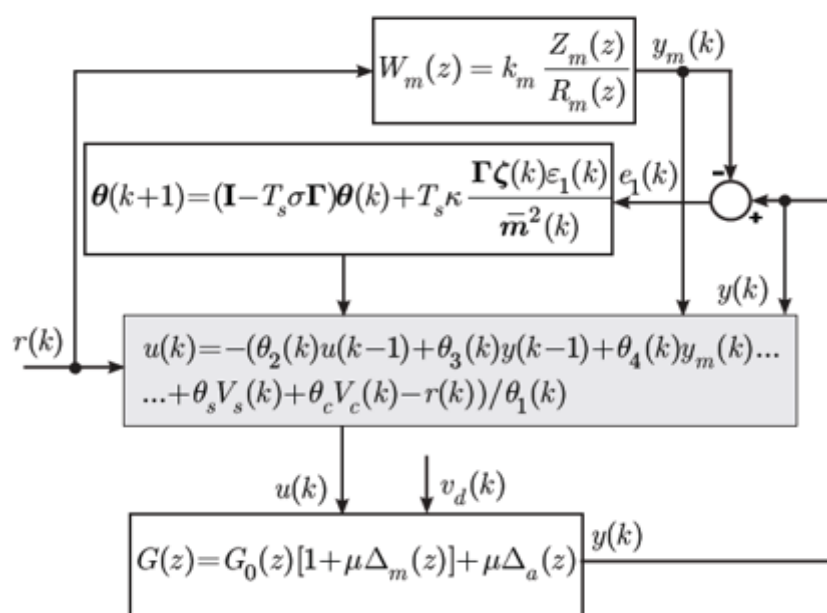


Fig. 3: Block diagram of control and adaptive structure
Source: Authors

4 CONTROLLER DESIGN

In this section, a design example is given for a 5.2 kW three-phase grid-connected converter with LCL filter, whose parameters are presented in Table 1. The design project considers, as shown in the development of the control law section, a reduced model for the plant, which makes the stability and convergence of the system, a major challenge for the control law.

Table 1. System parameters

	Symbol	Parameters	Value
Base Values	V_{cc}	DC link	400V
	vd	Grid voltage	127V
	f	Switching frequency	5kHz
LCL Filter	L_c	Converter-side inductance	1mH
	R_c	Converter-side resistance	50mΩ
	C	Capacitance of LCL Filter	62μf
	L_{gl}	Grid-side inductance	0.3mH
	R_{gl}	Grid-side resistance	50mΩ

Source: Authors

To implement the presented adaptive algorithm in a digital system, the following 9 steps are executed in a sampling period T_s :

- 1) Sampling of the PCC three-phase voltages, two-line AC currents in the converter side, two-line AC voltages in the capacitor, two-line AC currents in the grid and the voltage in DC link;

Then in $\alpha\beta$ coordinates:

- 2) Updating of the reference;
- 3) Updating of the reference model output;
- 4) Updating of $\zeta(k)$;
- 5) Updating of $\sigma(k)$;
- 6) Updating of augmented error;
- 7) Updating of the normalizing signal;
- 8) Updating of control action;
- 9) Updating of control gains vector.

Thus, in each sampling time the action control $u(k)$ is calculated for the modulation of the converter, in abc coordinates. By using the parameters presented in Table 1, the resulting transfer function is given by:

$$G(s) = \frac{i_g(s)}{u(s)} = \frac{5.376 \times 10^{10}}{s^3 + 216.7s^2 + 6.99 \times 10^7 s + 5.376 \times 10^9} \quad (23)$$

In order to simplify the development and design of the control structure it's considered simplified first order plant whit dynamics at the frequencies of interest (low frequencies), as described in the controller structure Eq. 6, where the LCL resonance peak is disregarded in the simplified plant. The equation representing the simplified plant is expressed as

$$G_0(s) = \frac{7.69257 \times 10^2}{s + 76.9257} \quad (24)$$

The LCL filter can be modeled as a first order equation without loss of performance, as shown in Evald et al. (2020). The Fig. 4 show the bode diagram of the simplified plant and real plant

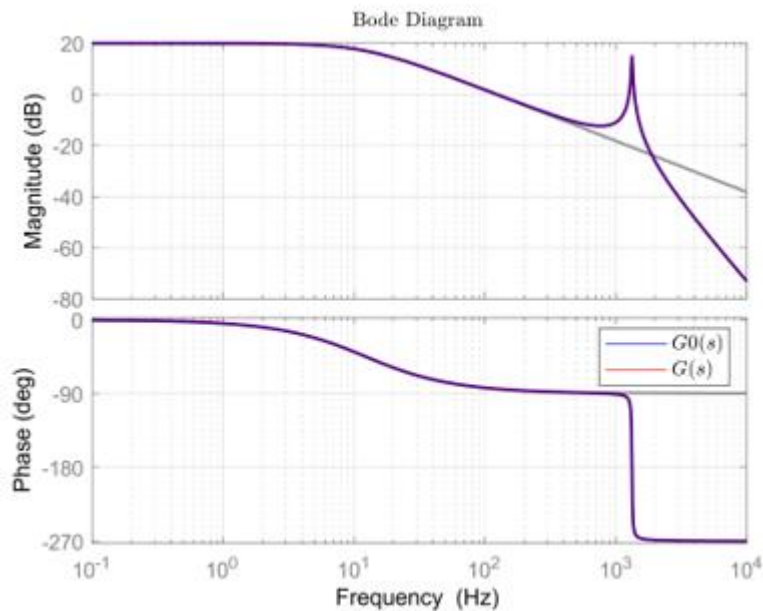


Fig. 4: Bode plot of G₀(s) (simplified dynamic plant) and G(s) (completed dynamic plant)
Source: Authors

Thus, considering the simplified plant, the model reference, can also be first order which is chosen as:

$$Wm(s) = \frac{1507}{s + 1507} \quad (25)$$

That is discretized with a sampling time of Ts = 1/5000

$$Wm(z) = \frac{0.2602}{z - 0.7398} \quad (26)$$

The reference r(k) of grid-current injected chosen for this project was a sinusoidal signal with 10A, 60Hz, 0° of Amplitude, Frequency and Phase respectively. Furthermore, in order to evaluate control performance, a 1mH inductance with 50mΩ of parasitic

resistance, in series with the grid is triggered at a certain instant, causing a parametric variation over the grid impedance.

The bode diagram, Figure 5 shows the open loop frequency response of the reference model, and the plant transfer function considering a parametric variation of grid-side inductance L_{g2} from 0.3mH to 1mH. Note that the position of the resonant peak changes because the position of the poles and zeros depend on the grid impedance. However, the close-loop poles are defined to be located at the same place even with parametric uncertainty or variation. Hence, the gains are adaptly changed to ensure this behavior.

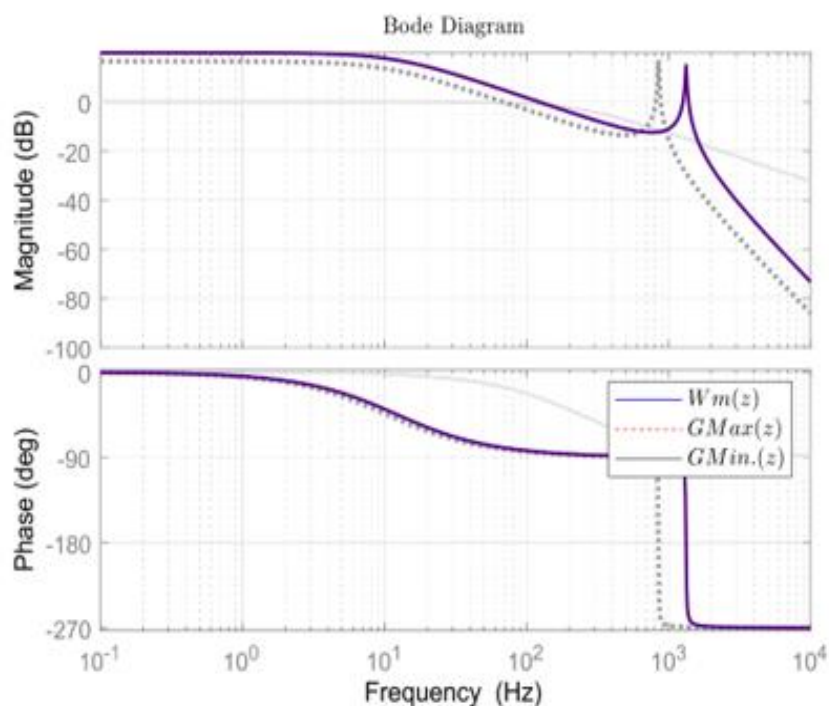


Fig. 5: Bode plot of $W_m(z)$ (desired closed-loop system) and of $G(z)$ (open loop plant) for different grid inductance

Source: Authors

In practice, before starting the close-loop operation, some control parameters must be initialized. As it is possible to have some idea about the grid impedance at the PCC, the initial gains $\theta(0)$ can be found from the matching condition Poh Chiang Loh and Holmes (2005) by assuming, for instance, the parameter L_{g2} with the nominal value as in Table 1.

The Table 2 presents the initial values and definitions of design controller

Table 2. Design controller parameters

Symbol	Value
$\theta(0)$	$[-1 \ 0 \ 0 \ 0 \ 0]$
Γ	10
κ	60
σ_0	0.1
M_0	15
\bar{m}^2	4
δ_0	0.7
δ_1	1
$\zeta(0)$	$[0 \ 0 \ 0 \ 0 \ 0]$

Source: Authors

5 SIMULATIONS RESULTS

In this section, some simulation results are given to demonstrate the performance of the proposed controller that was implemented in PSIM software for grid current control of the three-phase with LCL Filter, as shown in Figure 1.

The dynamic system and controller parameters are presented in Table 1 and 2 respectively, however, to avoid a large transient response, controller gains $\theta(0)$, in $\alpha\beta$, were initiated and chosen as the final values of a previous simulation, to avoid excessive overshoot in the initial transitory regime, while gains are adapting. It is highlighted that the only gain that must be initialized with correct signal is $\theta_1(0)$, to avoid division by zero. These gains are:

$$\theta_{\alpha}(0) = \begin{bmatrix} -0.73565596 \\ 0.25063896 \\ -0.38088176 \\ 0.042796385 \\ 0.086722091 \\ 0.42407233 \end{bmatrix} \text{ and } \theta_{\beta}(0) = \begin{bmatrix} -0.74094743 \\ 0.23399849 \\ -0.52122390 \\ -0.51915631 \\ 0.063335113 \\ 0.52586472 \end{bmatrix}$$

The Figure 6 shows the adaptation of the gains, to values shown below, in the α and β axis, during the initialization of the system:

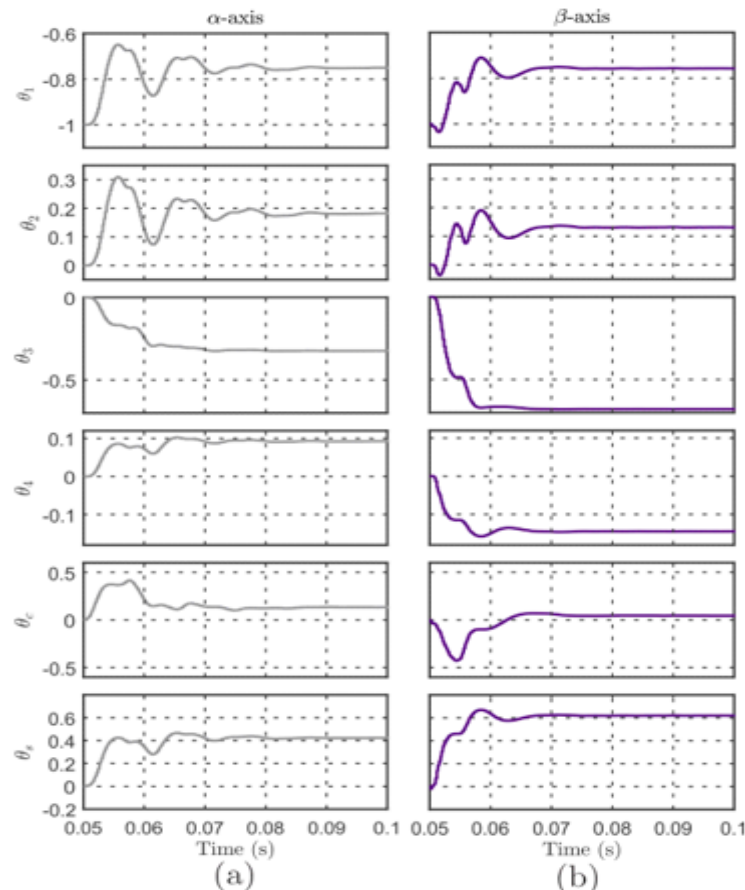


Fig. 6: Adaptation of the gains during initialization. (a) α -axis, (b) β -axis
Source: Authors

The Figures 7 and 8 show, in $\alpha\beta$ -axis, the output of plant and the reference model (y and y_m), the control action (u), the augmented and tracking error (ϵ_1 and e_1). The controller performance can be checked against initial transient response, parametric variation and amplitude variation.

- At $t = 0$ second, the synchronization of the converter with the grid is initialized. At $t = 0,05$ seconds, the converter starts the operation with active power reference current.

- At $t = 0,15$ second, a transient response occurs for a parametric variation in grid-side inductance L_{g2} , from 0,3mH to 1mH. Note that the controller has a good transient response.

- At $t = 0,2$ second, a transient response due to an active power step reference current change from 10A to 20A. It can be seen that the tracking and augmented errors have a reasonable transient response, against this abrupt variation in the current reference. The controller is capable to deal with it and the gains have converged to values close to θ^* making the output of the plant follow the output of the reference model, taking the error to zero in steady state. After $t = 0,3$ second, the amplitude reference current is set to 10A again.

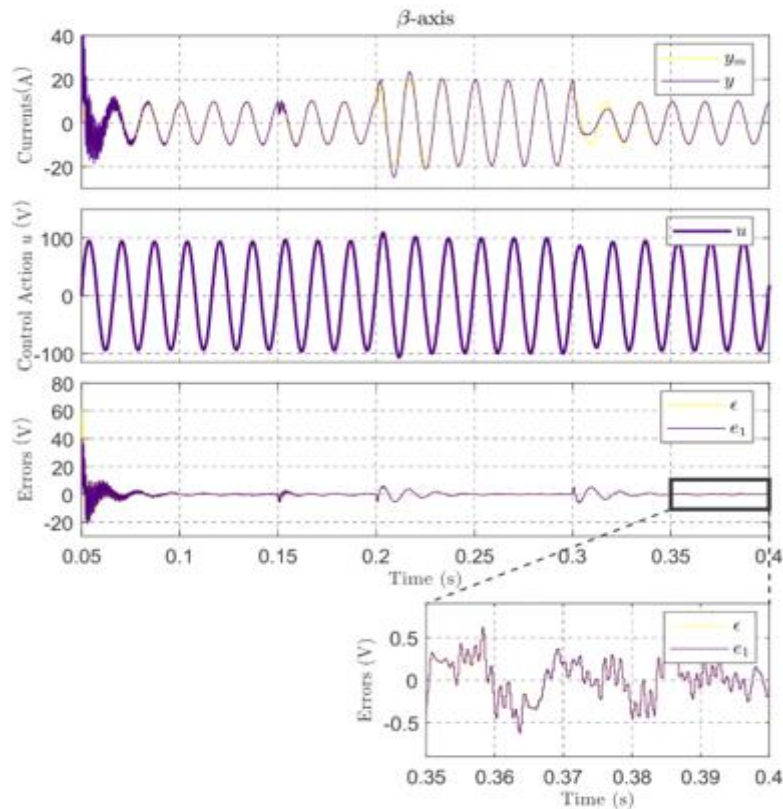


Fig. 7: Simulation Results. Transient response of parametric and amplitude variation in α axis
Source: Authors

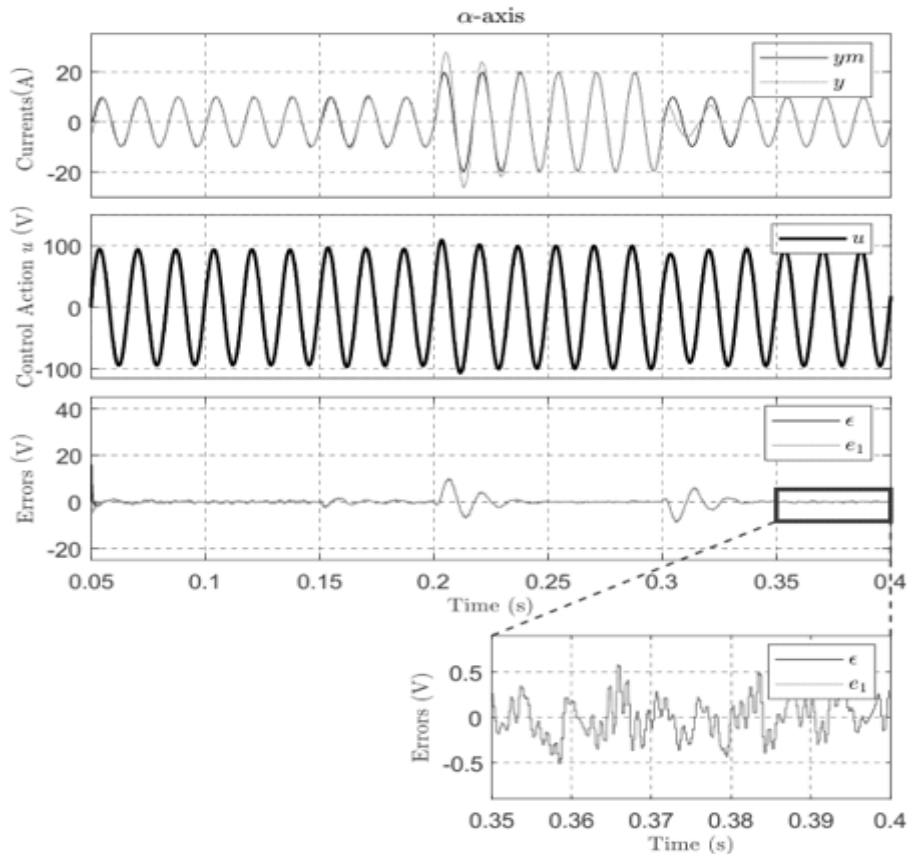


Fig. 8: Simulation Results. Transient response of parametric and amplitude variation in β axis
Source: Authors

The Figure 9 shows the adaptation of the gains during the startup. It can be reported that there is not a large variation in gains in the initial transient response, due to controller starts with adapted gains. Furthermore, it's possible to notice a similarity in the adaptation of the gains in the α and β axis. As for the characteristics and intrinsic structure of the controller, there is a greater effort to adapt gains to a variation in the amplitude of the reference current compared to parametric variation.

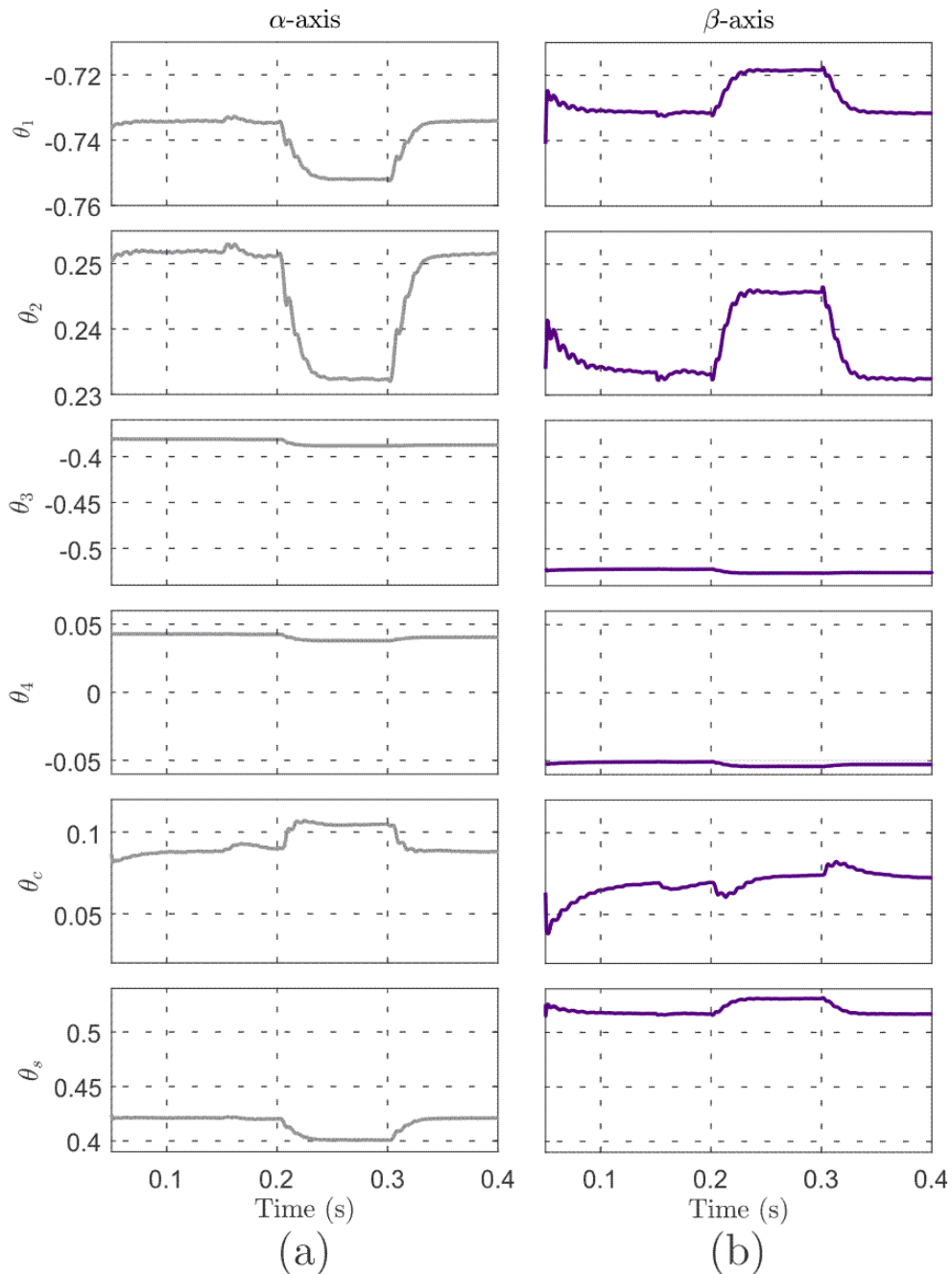


Fig. 9: Simulation Results. Adaptation of the feedback gains during the startup. (a) α -axis, (b) β -axis

Source: Authors

The Figure 10 shows the currents in ABC coordinates for the example simulation proposed, it can check that the adaptive current controller for grid-connected converter application can ensure fast transient response and good steady-state performance, even without knowledge of the equivalent grid impedance at the PCC. Moreover, the current-controlled grid-connected converter with LCL filter has the fast response imposed by the reference model, which is not dependent on the grid.

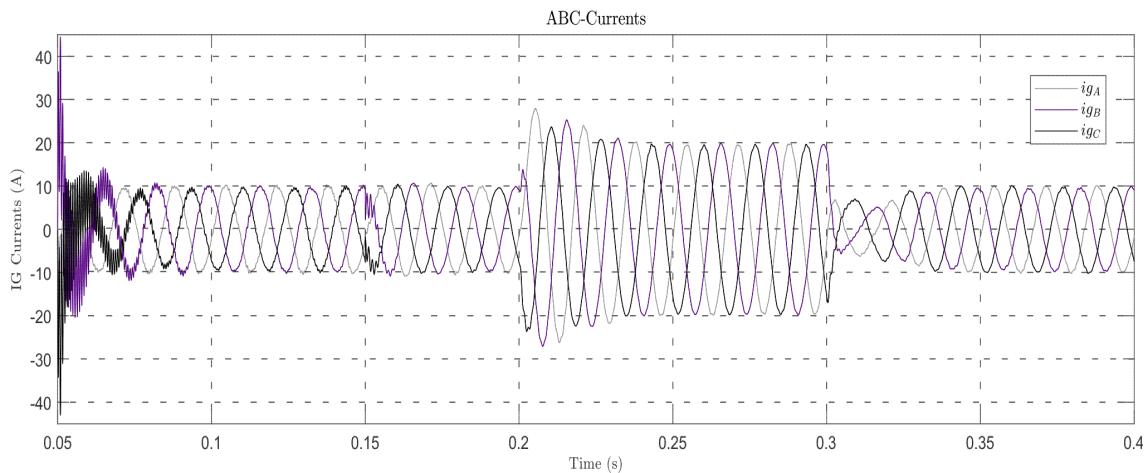


Fig. 10: Simulation results. Transient response of parametric and amplitude variation in ABC coordinates
Source: Authors

6 CONCLUSIONS

This paper presents a discrete-time adaptive current controller for grid-connected voltage source converters with LCL filter. It showed that the proposed adaptive algorithm provides a good performance in reference tracking as well as in disturbance rejection even under parametric variation and abrupt changes in the reference. The simulation results pointed out the effectiveness of the design procedure which it was main feature for the successful implementation of the adaptive controller.

ACKNOWLEDGMENT

To the Brazilian agencies CAPES and CNPq - Finance Code 001. CAPES 88887.479774/2020-00.

REFERENCES

- Baek, J., Kim, S., and Kwak, S. (2015). Predictive control method for load current of single-phase voltage source inverters. In 2015 IEEE Applied Power Electronics Conference and Exposition (APEC), 2256–2260.
- Chen, J.W., Liu, Y.C., et al. (2019). Design of dc micro- grid system for integration of pmsm elevator and renew- able energy sources. In 2019 IEEE 10th International Symposium on Power Electronics for Distributed Generation Systems (PEDG), 981–985. IEEE.
- Chowdhury, V.R. (2016). Analysis control and design of a hybrid renewable power generation system. In North American Power Symposium (NAPS), 1–7. IEEE.
- Costa, et. al. (2020). Energia solar fotovoltaica uma alternativa viavel? In Brazilian Journal Development, vol. 6. Number 9, 2020. DOI:10.34117/bjdv6n9-639
- Dannehl, J., Fuchs, F.W., and Hansen, S. (2007). PWM rectifier with LCL-filter using different current control structures. In 2007 European Conference on Power Electronics and Applications, 1–10. IEEE.
- Duesterhoeft, W.C., Schulz, M.W., and Clarke, E. (1951). Determination of instantaneous currents and voltages by means of alpha, beta, and zero components. Transactions of the American Institute of Electrical Engineers, 70(2), 1248–1255.
- Evald, P.J.D.O., Tambara, R.V., and Grundling, H.A., A direct discrete-time reduced order robust model reference adaptive control for grid-tied power converters with LCL filter.", Revista Eletrônica de Potência, vol. 25, number 3, 2020.
- Evald, et. Al (2020), A Discrete-Time Robust Adaptive PI Controller For Grid-Connected Voltage Source Converter With LCL Filter, Revista Eletrônica de Potência. (in press), 2021.
- Evald, P.J.D.O.; Tambara, R.V.; Gründling, H.A. (2020) A Discrete-Time Robust MRAC Applied on Grid-Side Current Control of a Grid-Connected Three-Phase Converter with LCL Filter. ELECTRIMACS 2019: Selected Papers-Volume 1, v. 615, p. 45, 2020.
- Exposto, B., Rodrigues, R., Pinto, J.G., Monteiro, V., Pedrosa, D., and Afonso, J.L. (2015). Predictive control of a current-source inverter for solar photovoltaic grid interface. In 2015 9th International Conference on Compatibility and Power Electronics (CPE), 113–118.
- Fang, X., Ding, X., Zhong, S., and Tian, Y. (2019). Improved quasi-y-source dc-dc converter for renewable energy. CPSS Transactions on Power Electronics and Applications, 4(2), 163–170.
- Gabe, I.J., Montagner, V.F., and Pinheiro, H. (2009). Design and implementation of a robust current controller for vsi connected to the grid through and lcl filter. IEEE Transactions on Power Electronics, 24(6), 1444 – 1452. Ioannou, P.A. and Tsakalis, K.S.

(1986a). A robust direct adaptive controller. *IEEE Transactions on Automatic Control*, 31(2), 1033 – 1043.

Hollweg, et. al. (2020). Controlador Robusto Adaptativo Super-Twisting Sliding Mode Por Modelo De Referência Para Regulação Das Correntes Injetadas Em Redes Fracas Por Inversores Trifásicos Com Filtro LCL, *Revista Eletrônica de Potência*, (in press), 2021.

Ioannou, P.A. and Tsakalis, K.S. (1986b). A robust discrete-time adaptive controller. *IEEE Proceedings of 25th Conference on Decision and Control*, (2), 1033 – 1043.

Jha, S. (2016). Implication of optimal performance of renewable energy system. In *7th Power India International Conference (PIICON)*, 1–5. IEEE.

Kuznietsov, M., Vyshnevskaya, Y., Brazhnyk, I., and Melnyk, O. (2019). Modeling of the generation-consumption imbalance in the heterogeneous energy systems with renewable energy sources. In *6th International Conference on Energy Smart Systems (ESS)*, 196–200. IEEE.

Lindgren, M. and Svensson, J. (1998). Control of a voltage-source converter connected to the grid through an lcl-filter-application to active filtering. *Proceedings of PESC'98*, 229 – 235.

Liserre, M., Teodorescu, R., and Blaabjerg, F. (2006). Stability of photovoltaic and wind turbine grid-connected inverters for a large set of grid impedance values. *IEEE Transactions on Power Electronics*, 21(1), 263–272.

Maccari, L.A.; Massing, J..S.L..R.C..P.H..O.R..F.M.V. (2014). Lmi-based control for grid-connected converters with lcl filters under uncertain parameters. *Power Electronics, IEEE Transactions on*, 29, 3776–3785.

Malinowski, M., Milczarek, A., Kot, R., Goryca, Z., and Szuster, J.T. (2015). Optimized energy-conversion systems for small wind turbines: Renewable energy sources in modern distributed power generation systems. *IEEE Power Electronics Magazine*, 2(3), 16–30.

Mariethoz, S., Beccuti, A.G., and Morari, M. (2008). Analysis and optimal current control of a voltage source inverter connected to the grid through an lcl filter. *Records of IEEE Power Electronics Specialists*, 2132 – 2138.

Massing, J., Stefanello, M., Gründling, H., and Pinheiro, H. (2012). Adaptive current control for grid-connected converters with lcl-filter. *Industrial Electronics, IEEE Transactions on*, 59, 4681 – 4693.

Mohamed, Y.R. and El-Saadany, E. (2007). An improved deadbeat current control scheme with a novel adaptive self-tuning load model for a three-phase PWM voltage-source inverter. *IEEE Trans. Ind. Electron.*, 54(2), 747– 759.

Poh Chiang Loh and Holmes, D.G. (2005). Analysis of multiloop control strategies for LC/CL/LCL-filtered voltage- source and current-source inverters. *IEEE Transactions on Industry Applications*, 41(2), 644–654.

Ponnaluri, S. and Serpa, L. (2008). Dc/ac converter with dampened lcl filter distortions. United States Patent, (US7450405B2).

Shi, H., Zong, J., and Ren, L. (2019). Modified model predictive control of voltage source inverter. In 2019 IEEE 4th Advanced Information Technology, Electronic and Automation Control Conference (IAEAC), volume 1, 754–759.

Tambara, R.V. (2014). Um controlador adaptativo robusto aplicado a conversores estáticos conectados à rede elétrica através de filtro LCL. Ph.D. thesis, Universidade Federal de Santa Maria, UFSM.

Tambara, R.V., Massing, J.R., Pinheiro, H., and Gründling, H.A. (2013). A digital RMRAC controller based on a modified RLS algorithm applied to the control of the output currents of an lcl-filter connected to the grid. European Power Electronics conference (EPE).

Tambara, R.V., Kanieski, J.M., Massing, J.R., Stefanello, M., and Gründling, H.A. (2017). A discrete-time robust adaptive controller applied to grid-connected converters with LCL filter. *Journal of Control, Automation and Electrical Systems*, 28(3), 371–379.